Journal of The Electrochemical Society, **146** (10) 3696-3701 (1999)
S0013-4651(99)01-025-3 CCC: $7.00

Structure and Function of Ferricyanide in the Formation of Chromate Conversion Coatings on Aluminum Aircraft Alloy

Lin Xia and Richard L. McCreery*

Department of Chemistry, The Ohio State University, Columbus, Ohio 43210, USA

Raman and infrared spectroscopy were used to determine the structure of $Fe(CN)_6^{-3}$ and its reaction products in chromate conversion coatings (CCCs) on AA 2024-T3 aluminum aircraft alloy. In addition, Raman spectroscopy was used to monitor CCC growth rates and their dependence on coating bath composition. The IR and Raman spectra of the air-dried CCC corresponded to those of Berlin green, a Fe^{+3}-CN-Fe^{+3} polymer, and $Fe(CN)_6^{-3}$ physisorbed on $Cr(OH)_3$. No other cyano-containing products were observed. When $Fe(CN)_6^{-3}$ was excluded from the coating bath, CCC formation rate greatly decreased. In addition, it was observed that $Fe(CN)_6^{-3}$ could rapidly oxidize AA 2024-T3, and $Fe(CN)_6^{-4}$ rapidly reduced Cr(VI) in bath conditions. These results indicate a redox mediation action for $Fe(CN)_6^{-3/-4}$, which greatly increases the reduction of Cr(VI) to Cr(III) by the alloy. This process is normally quite slow, and redox mediation by $Fe(CN)_6^{-3}$ is critical to CCC formation. $IrCl_6^{-3/-2}$ could substitute for $Fe(CN)_6^{-3/-4}$ to produce a chromate film with properties very similar to a conventional CCC. The results establish redox mediation as the mechanism of acceleration of CCC formation, but provide no evidence for any additional role of $Fe(CN)_6^{-3/-4}$ in corrosion protection.

Manuscript submitted January 11, 1999; revised manuscript received June 23, 1999.

Chromate conversion coatings (CCCs) have been used extensively to protect Cu-rich aluminum alloys, such as AA 2024-T3 aircraft alloy. As one of the essential components in the coating solution, ferricyanide is added as an "accelerator" due to the fact that it can increase the CCC film formation rate dramatically. Except for this well-known critical function in CCC formation, little is known about the acceleration mechanism of $Fe(CN)_6^{-3}$ and its possible role in CCC anticorrosion properties. It is known that $Fe(CN)_6^{-3/-4}$ is incorporated into the CCC film, and its role in corrosion inhibition has been considered. However, the specific nature of ferricyanide species in the CCC and the mechanism of "acceleration" are not clearly understood.

Various analytical techniques have been used on CCCs, including X-ray photoelectron spectroscopy (XPS),[1-6] X-ray absorption near-edge structure (XANES),[7,8] Fourier transform infrared spectroscopy (FTIR)[1,9] and Raman spectroscopy.[10] CCCs formed on 2024 or 7025 alloys by a commercial Alodine 1200S bath were found to contain Cr(VI),[a] Cr(III), iron, carbon, oxygen, and hydrogen, and small amounts of Cu and Al were found in the inner layer of the film.[1,3-5] A major Cr species in the CCC was spectroscopically identified as chromium-mixed oxide, in which Cr(VI) is chemically adsorbed to polymeric Cr(III) hydroxide through Cr(III)-O-Cr(VI) bonds.[9] Iron, carbon, and nitrogen were observed to be present in the CCC as Cr or Cu salts of ferricyanide, based on XPS and Auger electron spectroscopy (AES).[3,5,6]

The current work investigates the structure of Fe and cyanide species and the chemical role of ferricyanide in CCC film formation on a molecular level. Vibrational spectroscopy based on FTIR absorption and Raman scattering were chosen for several reasons. First, the CN stretch is both IR and Raman active, and its frequency (ν_{CN}) is quite sensitive to local bonding and counterion. For example, CN of $Cr_4[Fe(CN)_6]_3$ [11] and $K_4Fe(CN)_6$ differ by 54 cm^{-1}. Second, previous comprehensive structural studies of cyano-containing compounds by vibrational spectroscopy provide a "database" for structure characterization, and sophisticated theoretical models are available to predict CN vibration for certain rare or unstable cyano compounds.[11,12] Third, FTIR and Raman are generally nondestructive, and under some circumstances *in situ* Raman spectroscopy can provide structural information dynamically, during CCC formation.

Experimental

Prussian blue was prepared by adding 0.5 g $Fe(NH_4)(SO_4)_2 \cdot 12H_2O$ to 20 mL of 0.05 M $K_4Fe(CN)_6 \cdot 3H_2O$ solution [Fe(II):Fe(III)=1:1]. After brief stirring, the dark blue precipitate was collected and washed. Berlin green was prepared in a similar way, except that 20 mL of 0.05 M $K_3Fe(CN)_6$ solution was used. Fe^{+2}-CN-Cr^{+3} polymer was prepared by the method of Brown *et al.*[11] In a N_2 atmosphere, Cr^{+3} was reduced to Cr^{+2} with Zn metal, then $K_4Fe(CN)_6$ was added and stirred for 2 h. The nearly white precipitate was collected by filtration, then dried in air to a light yellow solid. Cu(II)-ferricyanide and Cu(II)-ferrocyanide were made by adding 0.9 g $K_3Fe(CN)_6$ or 1 g $K_4Fe(CN)_6 \cdot 3H_2O$ into 20 mL of 0.1 M $CuSO_4$ solution while stirring. The precipitate was collected and washed. $Fe(CN)_6^{-3}/Cr(OH)_3$ and $Fe(CN)_6^{-4}/Cr(OH)_3$ were prepared either simultaneously or sequentially. In the simultaneous method, ~2 g $Cr(NO_3)_3 \cdot 9H_2O$ and 0.5 g $K_3Fe(CN)_6$ or 0.7 g $K_4Fe(CN)_6 \cdot 3H_2O$ were dissolved in 20 mL of nanopure water, then 1 M NaOH was added dropwise while agitating the solution. The precipitate was collected at pH 5-7, then washed with Nanopure water. In the sequential method, $Cr(OH)_3$ was prepared from $Cr(NO_3)_3 \cdot 9H_2O$ and NaOH solutions, washed, then immersed in 0.05 M of $K_3Fe(CN)_6$ or $K_4Fe(CN)_6 \cdot 3H_2O$ solution, with agitation. The solid was collected by filtration. $Fe(CN)_6^{-3}/Al(OH)_3$ and $Fe(CN)_6^{-4}/Al(OH)_3$ were prepared by the simultaneous method as above, except that $Al(NO_3)_3 \cdot xH_2O$ ($x \sim 9$) replaced $Cr(NO_3)_3 \cdot 9H_2O$.

The test solutions for growth rate studies were prepared from nanopure water and analytical grade $K_2Cr_2O_7$, $K_3Fe(CN)_6$, NaCN, KBF_4, K_2ZrF_6, HNO_3, and $HClO_4$ with the final concentrations listed in Table I. Three AA 2024-T3 coupons (1 × 1 cm, in epoxy mounts) were polished[9] and coated in test solutions for 1, 3, or 5 min, then washed and dried in air before any further measurement. The volume of test solutions use for treatment was ~50 mL, and a given test solution was used for all three samples. AA 2024-T3 alloy made by Aluminum Company of America was obtained from Joseph T. Ryerson and Son, Inc.

Raman and FTIR spectra were obtained as described previously[9] except that IR spectra were obtained in reflection mode from coated surfaces.

Results

Structure of CN species in CCC.—The IR and Raman spectra of a CCC film and the peak assignment have been reported previously.[9] In addition to the Cr-O and OH vibrations, the IR spectrum shows a Fe-CN vibration at 592 cm^{-1} and a CN vibration at 2083 cm^{-1}. Raman spectra of the CCC show CN vibrations at 2098 and

* Electrochemical Society Active Member.

[a] The use of Roman or Arabic numerals to indicate oxidation state is somewhat inconsistent in the literature. We use Roman numerals to indicate oxidation state and Arabic numerals to indicate ionic charge, with the exception of mixed metal cyano compounds, where Roman numerals are cumbersome.

S0013-4651(99)01-025-3 CCC: $7.00

Table I. Components in test solutions for growth-curve studies.

Solution	Cr(VI) (mM) (from $K_2Cr_2O_7$)	NaF (mM)	NaCN (mM)	$K_3Fe(CN)_6$ (mM)	KBF_4 (mM)	K_2ZrF_6 (mM)	pH
A	42.2	14.4	0	0	0	0	1.6 (with HNO_3)
B	42.2	14.4	3	0	0	0	1.6 (with HNO_3)
C	42.2	14.4	0	3	0	0	1.6 (with HNO_3)
D	42.2	14.4	0	3	14.6	2	1.6 (with HNO_3)
Alodine	42.2[a] (38-45)[a]	14.4[a] (9-18)	0	2.5 (2-3)	15 (12-18)	1.5 (1-2)	1.6 (with HNO_3)

[a] Concentrations for commercial Alodine are assumed to equal average of range shown on material safety data sheet, shown in parenthesis.[22]

2145 cm^{-1} plus the prominent 858 cm^{-1} band attributed to the Cr(III)/(VI) mixed oxide. Some spectroscopic changes were observed when the CCC was aged in air or water. Figure 1 shows Raman spectra of a fresh CCC and one aged for 17 days in air or immersed in Nanopure water. Air exposure causes minor changes in the Raman spectrum, with a slight decrease in the H-O-H bend intensity (~1650 cm^{-1}) presumably due to dehydration. Water exposure causes a major decrease in the 858 cm^{-1} band, to about 12% of its original area, and some changes in the CN stretch region. With the large decrease in 858 cm^{-1} intensity, the Cr(III)-OH stretch at 528 cm^{-1} becomes visible. IR spectra (Fig. 2) also show little change during air aging, with some decrease in the 3400 cm^{-1} water band, and a significant decrease in the CN stretch intensity during aging in water. As shown in the insets in Fig. 2, the decrease in 2083 cm^{-1} IR absorption in water is associated with relative intensity changes in the two component bands at 2065 and 2089 cm^{-1}.

There are several possibilities for the form of CN and $Fe(CN)_6$ in the CCC film. Since the CN stretching frequency is quite sensitive to environment and bonding, it may be used as a fingerprint to compare the frequency observed in the CCC with that of known materials. Some of the possible forms of $Fe(CN)_6^{-3/-4}$ in the CCC include trapped or physisorbed $Fe(CN)_6^{-3}$ or $Fe(CN)_6^{-4}$, $Cu_2Fe(CN)_6$, $Cu_3[Fe(CN)_6]_2$, salts of Cr(III) and $Fe(CN)_6^{-3}$ or $Fe(CN)_6^{-4}$, and the degradation products resulting from $Fe(CN)_6^{-3}$ hydrolysis. The latter include Prussian blue (Fe^{+3}-CN-Fe^{+2}) and Berlin green (Fe^{+3}-CN-Fe^{+3}). [13] These are polymeric species with cyano bridges between iron centers and are insoluble in water. As noted in the Experimen-

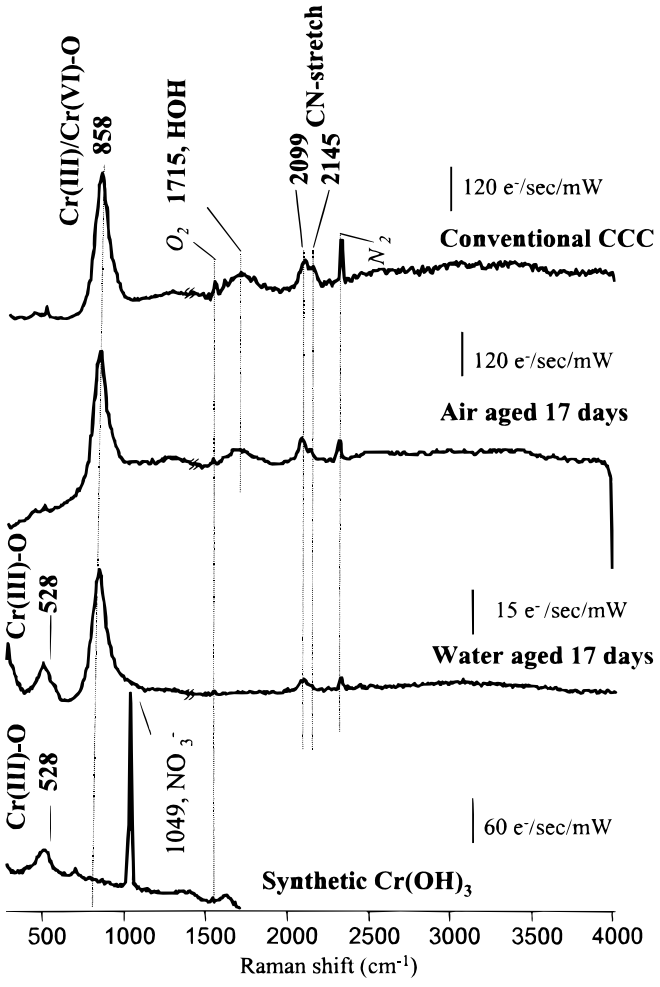

Figure 1. Raman spectra of fresh CCC film (aged 0.5 h), CCC after aging in air at room temperature for 17 days or after immersion in nanopure water for 17 days, 514.5 nm laser, ~15 mW at sample, integration time was 30 s, average of 5-10 integrations. Spectra were acquired in two segments, 300-1400 cm^{-1} and 1400-4000 cm^{-1}. Sharp features at 518, 1555, and 2331 cm^{-1} are due to stray room light, atmospheric O_2 and N_2, respectively.

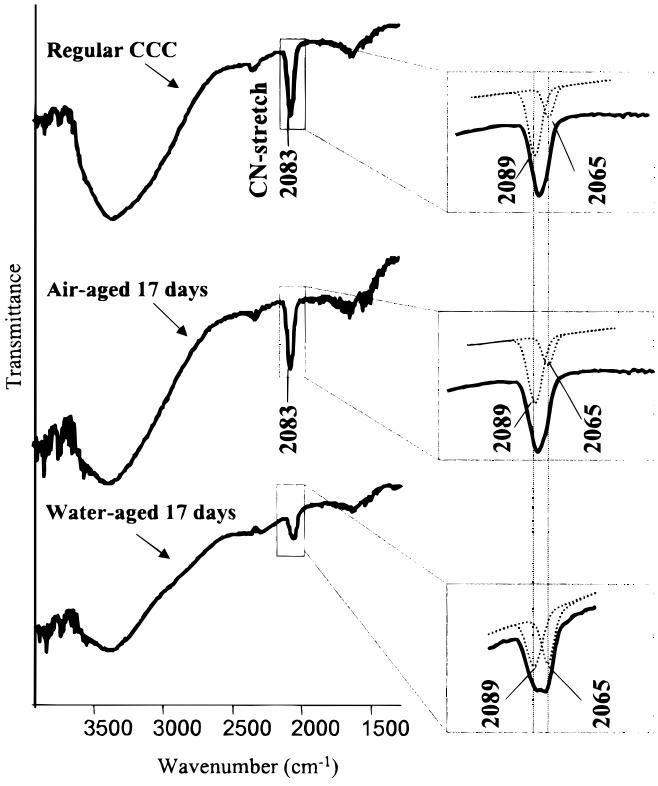

Figure 2. FTIR spectra of fresh CCC aged 0.5 h, and after aging in air or water for 17 days. Spectra were obtained in reflection mode. 300 scans were co-added before Fourier transform. Dotted lines are deconvolution results.

S0013-4651(99)01-025-3 CCC: $7.00

tal section, Prussian blue and Berlin green are easily prepared by precipitating aquated Fe^{+3} with either $Fe(CN)_6^{-4}$ or $Fe(CN)_6^{-3}$.

Raman spectra of the CN stretch region of several synthetic salts of ferri- and ferrocyanide are compared to that of a CCC in Fig. 3. FTIR spectra of the same materials show a single C≡N stretch feature, and the observed Raman and IR frequencies are listed in Table II. The IR and Raman ν_{CN} frequencies of CCC do not match those of $K_4Fe(CN)_6$, $K_3Fe(CN)_6$, Berlin green, or Prussian blue, except for the close correspondence of the Berlin green IR frequency (2089 cm^{-1}) and one of the CCC IR bands (2089 cm^{-1}). However, incorporation of $Fe(CN)_6^{-3}$ into $Cr(OH)_3$ by either the sequential or simultaneous syntheses yields Raman features at 2098, 2132, and 2145 cm^{-1}. Raman spectra of $Fe(CN)_6^{-3}$ adsorbed onto synthetic Cr(III)/Cr(VI) mixed oxide[9] showed identical CN stretch frequencies. These match the Raman bands of the CCC (2099, 2145) and free $Fe(CN)_6^{-3}$ (2132). IR spectra of the $Fe(CN)_6^{-3}/Cr(OH)_3$ sample show a CN stretch at 2065 cm^{-1}, the same as the IR band observed for the CCC (2065 cm^{-1}). Therefore, the CN stretching features in the air-dried CCC correspond to $Fe(CN)_6^{-3}$ physisorbed on $Cr(OH)_3$ for the Raman spectra, and to Berlin green plus physisorbed $Fe(CN)_6^{-3}$ for the IR spectra. The Raman band for Berlin green at 2152 cm^{-1} is apparently too weak to observe in the CCC Raman spectrum, although its IR absorption (2089 cm^{-1}) is quite strong. Note also that depletion of Cr(VI) from the CCC by water exposure [with accompanying loss of the 858 cm^{-1} Cr(VI) band] results in Raman and IR spectra

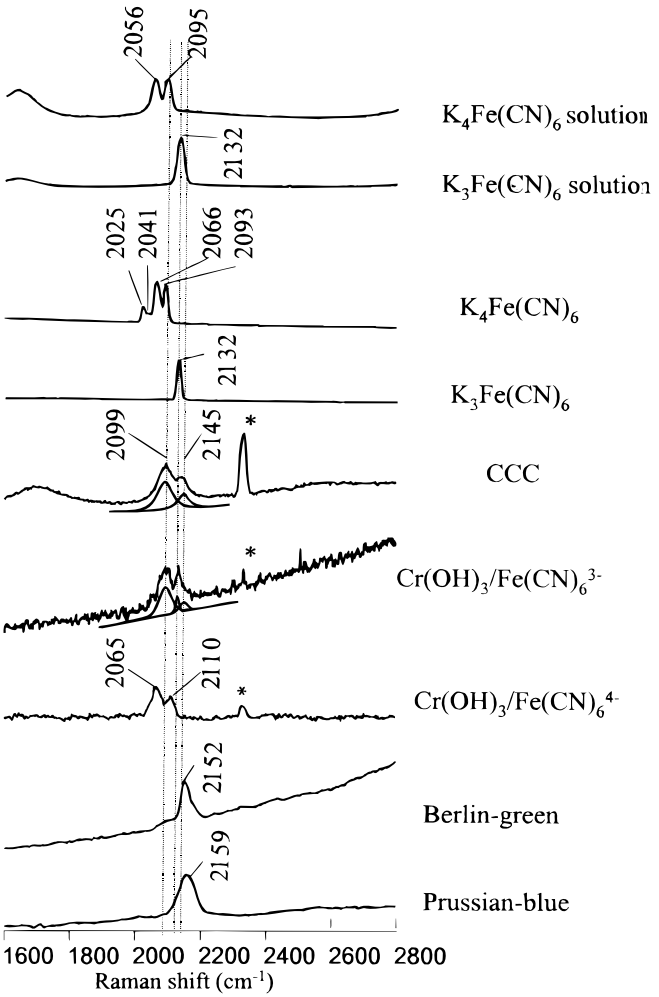

Figure 3. Raman spectra of various reference materials and CCC. Except for the top two, all samples were solids, 514.5 nm laser, 15 mW at sample, integration time was 30 s, all are average of 5-10 scans. Asterisks indicate signals from atmospheric N_2.

Table II. CN stretching frequencies of $Fe(CN)_6^{-3/-4}$ derivatives.

	ν_{IR}, cm^{-1} (This work)	ν_{Raman}, cm^{-1} (This work)
$K_3Fe(III)(CN)_6 \cdot 3H_2O$, solid	2118	2132
$K_4Fe(II)(CN)6 \cdot 3H_2O$, solid	2044	2025, 2066, 2093
Berlin green	2089 (strong)	2152 (weak)
Prussian blue	2078 (strong)	2159 (weak)
CCC (air, 17 days)	2083	2099, 2145
CCC (water, 17 days)	2065, 2089	~2099, ~2145 (very weak)
$Cr(OH)_3$ + $Fe(III)(CN)_6^{-3}$	2065	2098, 2132, 2145
$Cr(OH)_3$ + $Fe(II)(CN)_6^{-4}$		2067, 2110
$Al(III)(OH)_3$ + $Fe(III)(CN)_6$	2133	
$Al(III)(OH)_3$ + $Fe(II)(CN)_6$	2058	
$[Cu(II)]_3[Fe(III)(CN)_6]_2$	2100 (strong), 2172 (weak)	2188
$[Cu(II)]_2Fe(II)(CN)_6$	2098	2116, 2153

consistent with Berlin green and $Fe(CN)_6^{-3}$ physisorbed on $Cr(OH)_3$. Finally, it was possible to generate Berlin green, with its characteristic 2089 cm^{-1} cyano IR absorption, by slow hydrolysis of $K_3Fe(CN)_6$ at pH 1-1.5, in the presence of an excess of an oxidizing agent, $Na_2S_2O_8$. Therefore, the 2089 cm^{-1} IR feature may be produced without the involvement of chromium species.

Other combinations of Fe, Cu, Cr, CN^-, and $Fe(CN)_6^{-3}$ or $Fe(CN)_6^{-4}$ were considered, but did not correspond to observed CCC features. In particular, the $Al(OH)_3$ + ferri- or ferrocyanide and Cu(II) ferri/ferrocyanide salts listed in Table II do not match the observed CCC features. Additional cyano frequencies from the literature are listed in Table III, for several relevant metal/cyano combinations. For mixed metal complexes such as Cr^{+3}-CN-Fe^{+2}, the material can exist as isomeric Fe^{+2}-CN-Cr^{+3}, with a different ν_{CN}. In the case of the Fe^{+3}-CN-Cr^{+3} isomers, experimental values of ν_{CN} were unavailable, but well-established molecular mechanics calculations predict ν_{CN} values higher than $Fe(CN)_6^{-3}$ itself.[12] IR absorption for Fe^{+2}-CN-Cr^{+3} polymer (2098 cm^{-1}) is close to the CCC values of 2083 (wet) and 2089 (dry), but not as close as Fe^{+3}-CN-Fe^{+3} (2089 cm^{-1}). Cr^{+3} complexes of this type are slow to form due to the substitution inertness of Cr^{+3}.[11] Furthermore, Fe^{+2}-CN-Cr^{+3} should be susceptible to oxidation by Cr(VI) and should be unstable in the CCC. Finally, the IR spectrum of synthetic Fe^{+2}-CN-Cr^{+3} polymer prepared as described in the literature[11] showed a ν_{CN} of 2097 cm^{-1}. While other cyano complexes are possible, particularly as minority species, the spectroscopic results are consistent with physisorbed $Fe(CN)_6^{-3}$ and Berlin green (Fe^{+3}-CN-Fe^{+3} polymer) produced by partial hydrolysis of $Fe(CN)_6^{-3}$ during CCC formation.

To summarize the structural results, the observed IR and Raman spectra of the CCC on AA 2024-T3 indicate the formation of Berlin green (Fe^{+3}-CN-Fe^{+3} polymer) and physisorption of $Fe(CN)_6^{-3}$ to the polymeric $Cr(OH)_3$ matrix. Prolonged exposure to water (17 days) causes a loss of 80-90% of the Cr(VI) in the CCC, and leaves behind insoluble $Cr(OH)_3$ polymeric backbone containing Berlin green and $Fe(CN)_6^{-3}$. If cyano compounds other than Berlin green and physisorbed $Fe(CN)_6^{-3}$ are present in the CCC, they were not observed with either FTIR or Raman spectroscopy.

Function of $Fe(CN)_6^{-3}$ during CCC formation.—Now that the major products of $Fe(CN)_6^{-3}$ in the CCC are identified, we turn to the question of the role of $Fe(CN)_6^{-3}$ in CCC formation. It is well known that $Fe(CN)_6^{-3}$ increases the rate of CCC formation on aluminum alloys, hence the term "accelerator". The effect is shown clearly in Fig. 4, which shows the growth of the 858 cm^{-1} band of the CCC as a function of immersion time in various bath solutions. The commercial Alodine bath contains Cr(VI) (38-45 mM), NaF (9-18 mM),

S0013-4651(99)01-025-3 CCC: $7.00 © The Electrochemical Society, Inc.

Table III. Literature values for cyano stretch of several metallocyanide compounds.

Compound	ν_{CN} (IR) observed	ν_{CN} (IR) calculated	ν_{CN} (Raman) observed
Cr^{+3}-CN-Fe^{+2}	2170 [11]	—	N/A
Cr^{+3}-CN-Fe^{+3}	N/A	>2128 [a]	N/A
Fe^{+2}-CN-Cr^{+3}	2098 [11]	—	N/A
	~2090 [14]		
	2097 [b]		
Fe^{+3}-CN-Cr^{+3}	N/A	>2118[a]	N/A
$K_4Fe(CN)_6 \cdot 3H_2O$ solid for IR	2044 [15]	—	
$K_4Fe(CN)_6$ solution for Raman	2044 [12]		2094, 2058 [18]
	2044 [16]		2098, 2062 [20]
	2044 [17]		2098, 2062 [17]
	2044 [20]		
$K_3Fe(CN)_6 \cdot 3H_2O$ solid for IR	2118 [4]		2131 [19]
$K_3Fe(CN)_6$ solution for Raman	2118 [20]		2135 [20]
	2118 [16]		2132 [18]
			2132 [21]
Cr(III)-CN	2128 [12]	—	N/A
Cu(II)-CN	2125 [12]	—	N/A
Cu(I)-CN	2094 for $Cu(CN)_3^{2-}$ [12]	—	N/A
	2076 for $Cu(CN)_4^{3-}$ [12]		
Free CN- (aqueous)	2080 [15]	—	N/A
	2080 [12]		

[a] Calculated as described in Ref. 12, p. 111.
[b] Obtained for material synthesized during the current work.

$Fe(CN)_6^{-3}$ (2-3 mM), KBF_4 (12-18 mM), and K_2ZrF_6 (1-2 mM). The exact concentrations are proprietary, and the bath solution is normally adjusted to pH 1.6 with HNO_3. [22] Synthetic coating solutions were prepared from reagent grade chemicals with concentrations approximately equal to those in Alodine, but with one or more reagents omitted (Table I). Figure 4 shows the growth of the 858 cm^{-1} band on AA 2024-T3 for several of these synthetic solutions, all at room temperature. KBF_4 and K_2ZrF_6 have little effect on film growth, and $HClO_4$ may be substituted for HNO_3 with no apparent effect. Growth is much slower if $Fe(CN)_6^{-3}$ is omitted, with the 858 cm^{-1} Raman band reaching a level only a few percent of its value for the Alodine solution. CN^- itself did not accelerate growth in the absence of $Fe(CN)_6^{-3}$, so free CN^- resulting from $Fe(CN)_6^{-3}$ decomposition does not appear sufficient for rapid film growth. Similar behavior was observed for 99.999% aluminum (Fig. 5), although the deposition rate in the absence of $Fe(CN)_6^{-3}$ was faster than that observed for AA 2024-T3. The open-circuit potential of pure Al is significantly negative of that of 2024 during CCC formation, which may explain the more rapid reduction of Cr(VI) on pure Al in the absence of $Fe(CN)_6^{-3}$. The Raman spectra for the CCC films grown in solutions containing $Fe(CN)_6^{-3}$ are shown in Fig. 6 and indicate that the absence of BF_4^-, ZrF_6^{-2}, or NO_3^- does not lead to spectroscopically observable changes in film structure. Taken as a whole, the results depicted in Fig. 4-6 lead to the conclusion that the true "accelerator" is either $Fe(CN)_6^{-3}$ itself or one of its degradation products, such as Berlin green or Prussian blue.

In the current context, a redox mediation mechanism would be possible if the direct reduction of Cr(VI) to Cr(III) by the alloy were

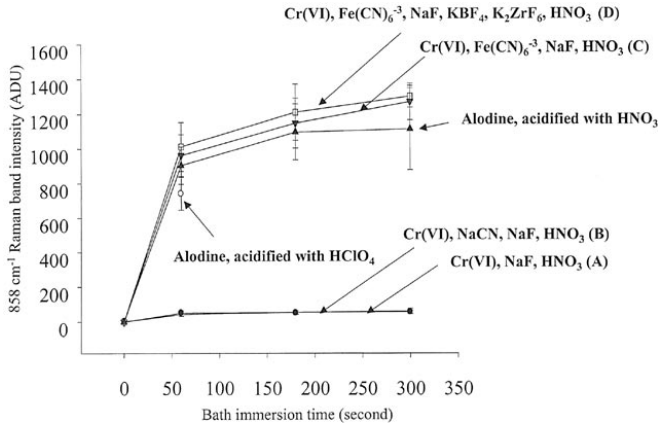

Figure 4. Growth curves of 858 cm^{-1} Raman peak intensity on AA 2024-T3 in various test solutions. Letters in parentheses refer to compositions listed in Table I. To obtain the curves, 6-10 Raman spectra from different spots on one treated coupon were collected, with a 514.5 nm laser, 2.5 mW at sample, 1 s integration. The average of the 6-10 858 cm^{-1} band intensities is plotted as the ordinate, with the error bars indicating the standard deviation. All samples were washed thoroughly and dried briefly after treatment.

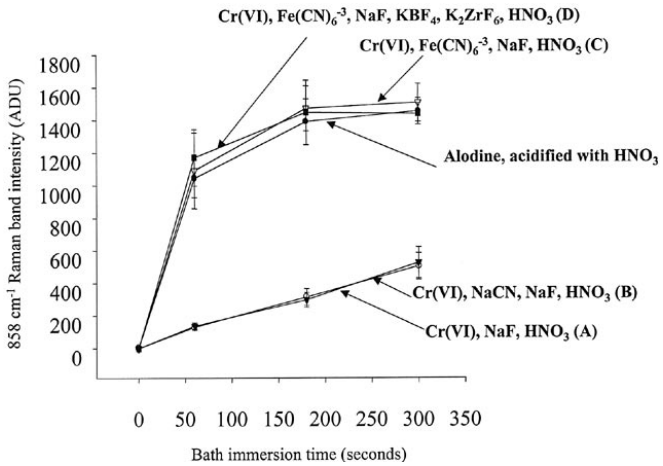

Figure 5. Growth curves of 858 cm^{-1} Raman peak intensity on 99.999% pure aluminum. All conditions are the same as Fig. 4.

S0013-4651(99)01-025-3 CCC: $7.00

quite slow. Figure 4 provides strong evidence that this is the case, since CCC growth is very slow in the absence of $Fe(CN)_6^{-3/-4}$, indicating a slow reduction of Cr(VI) by the aluminum or alloy surface. For redox mediation to increase the reduction rate, the reduced form of the mediator must reduce Cr(VI) rapidly, and the alloy must reduce the oxidized form of the mediator rapidly, as shown schematically in Fig. 7. If both of these reactions are fast compared to direct reduction of Cr(VI) by the alloy, the overall reduction rate of Cr(VI) is increased in the presence of the mediator. The resulting rapid formation of Cr(III) results in more rapid CCC growth. The possibility that $Fe(CN)_6^{-3/-4}$ or Berlin green/Prussian blue may act as redox mediators was tested by observing their reactivity toward Cr(VI) and AA 2024-T3. Ferri- and ferrocyanide are easily distinguishable by Raman spectroscopy (Fig. 3), so relative concentrations may be monitored in solution. First, 6 mM $Fe(CN)_6^{-4}$ was rapidly and completely (<30 s) oxidized by 6 mM $Cr_2O_7^{-2}$. Second, polishing AA 2024-T3 in $Fe(CN)_6^{-3}$ solution for 2 min generated $Fe(CN)_6^{-4}$ in the solution. In addition, immersion of AA 2024-T3 in a solution of $Fe(CN)_6^{-3}$/NaF/HNO_3 (pH 1.6) for 20 min also generated $Fe(CN)_6^{-4}$. These experiments were performed in the same conditions as Alodine treatment, in which direct oxidation of AA 2024-T3 by Cr(VI) is very slow with $Fe(CN)_6^{-3}$ absent. Similar experiments were performed with the Berlin green/Prussian blue redox system with quite different results. Prussian blue was not detectably oxidized by 6 mM Cr(VI) upon stirring for 24 h. Polishing AA 2024-T3 in a solution saturated with Berlin green showed no reduction to Prussian blue. These experiments demonstrate that the redox mediation scheme depicted in Fig. 7 is feasible for $Fe(CN)_6^{-3/-4}$ but much less likely for Berlin green or Prussian blue. Since the kinetics will depend strongly on local concentrations and mass transport in the solution near the CCC, the observations do not permit detailed kinetic analysis. However, it is clear that the two redox cross reactions in Fig. 7 are much faster than direct reduction of Cr(VI) by AA 2024-T3. Of all species known to be present during CCC formation, $Fe(CN)_6^{-3/-4}$ is the only one which fulfills the requirements of a redox mediator. Furthermore, the acceleration of CCC growth on 99.999% aluminum, and the spectroscopic similarity of the resulting film imply that a similar mediation mechanism applies on pure Al as well as AA 2024-T3.

In principle, any redox system with a redox potential between that of Cr(VI)/Cr(III) and Al/Al(III) which also has fast redox kinetics with these two systems should be able to act as a mediator or accelerator. The Cr(VI)/(III) and Al/Al(III) potentials vary significantly with local conditions, but are approximately 2.0 V apart under Alodine conditions. $IrCl_6^{-3/-2}$ ($E° = +1.02$ V *vs.* NHE), $Fe^{+3/+2}$

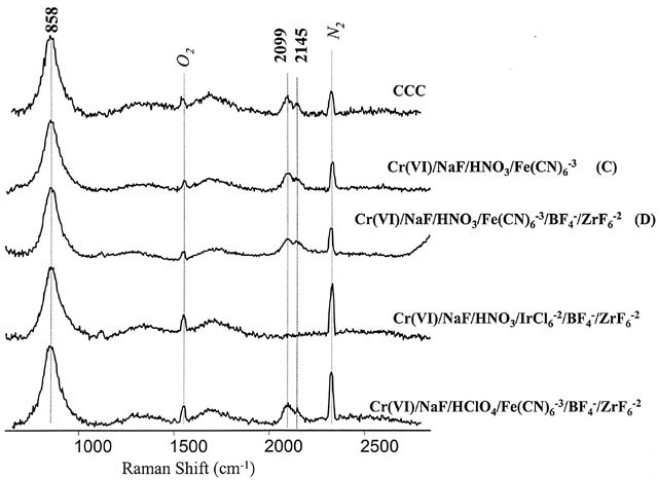

Figure 6. Raman spectra of CCC on AA 2024-T3 obtained by immersing it in commercial Alodine coating bath (top), model solution C (second), test solution D (third), and test solution D with $Fe(CN)_6^{-3}$ replaced by $IrCl_6^{-2}$ (fourth), and solution D with HNO_3 replaced by $HClO_4$ (bottom).

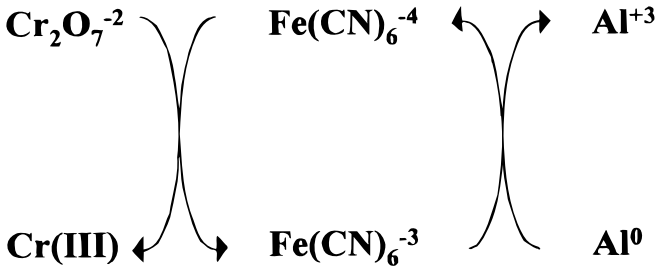

Figure 7. Proposed $Fe(CN)_6^{-3}$ mediation mechanism. Arrows represent redox cross reactions.

($E° = +0.77$ V), V^{+3}/V^{+2} ($E° = -0.26$) have redox potentials in the required range (compared to $Fe(CN)_6^{-3/-4}$ at +0.36 V *vs.* NHE), and were tested as mediators. Growth curves for the 858 cm^{-1} band are shown in Fig. 8 for solutions in which one of these mediator candidates was substituted for $Fe(CN)_6^{-3}$. Fe^{+3}, V^{+3}, and $IrCl_6^{-2}$ all accelerated CCC growth, although not as well as $Fe(CN)_6^{-3}$. The chromate films formed when $IrCl_6^{-2}$ was substituted for ferricyanide had Raman spectra very similar to those of the conventional CCC, except for the lack of CN features (Fig. 6). Furthermore, other properties of the film formed with $IrCl_6^{-2}$ are similar to a conventional CCC. The $IrCl_6^{-2}$ film releases soluble Cr(VI) like a CCC, and protects AA 2024-T3 from visual corrosion in 0.1 M NaCl. The polarization resistance increases from $<10^4$ to $>5 \times 10^5$ Ω cm^2 upon formation of the $IrCl_6$ catalyzed film. Finally, the film formed with $IrCl_6^{-2}$ can protect a nearby sample of untreated AA 2024 alloy from visible corrosion in the "artificial scratch" experiment.[23]

Discussion

The principal structural conclusions available from the Raman and IR results are that the CCC contains $Fe(CN)_6^{-3}$ adsorbed to $Cr(OH)_3$, and Berlin green, a complex hydrolysis product containing Fe^{+3} bridged by CN^- groups. The CN stretching frequency, ν_{CN}, for pure Berlin green is similar to that for Berlin green in the CCC, implying that the solid hydrolysis product is coprecipitated in the $Cr(OH)_3$ without strong interactions with the $Cr(OH)_3$ matrix. However, the shift in ν_{CN} downward by 35 cm^{-1} when $Fe(CN)_6^{-3}$ is adsorbed on $Cr(OH)_3$ implies a fairly strong interaction. Experimental and theoretical evidence has been reported for similar ν_{CN} shifts in compounds of the type X-CN- - - H-O-Y, where X and Y are either inorganic or organic molecules. Such interactions weaken the C≡N bond by redistribution of electron density, thus lowering ν_{CN}.[24-28] Therefore, the observed vibrational spectra support the conclusion that much of the cyano species in the CCC is in the form of $Fe(CN)_6^{-3}$ hydrogen bonded to Cr-OH groups in the $Cr(OH)_3$ matrix.

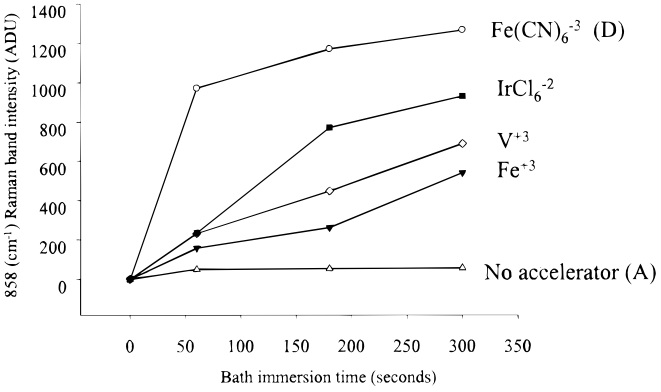

Figure 8. Growth curves of 858 cm^{-1} Raman peak on AA 2024-T3 in solution A (no accelerator), solution D (top) or solution D with $Fe(CN)_6^{3-}$ replaced by 3 mM $IrCl_6^{-2}$, V^{+3} or Fe^{+3}. All other conditions are the same as Fig. 4.

S0013-4651(99)01-025-3 CCC: $7.00

The additional cyano component of the CCC is Berlin green, with the generic structure Fe^{+3}-CN- Fe^{+3}. Berlin green is a three-dimensional lattice with Fe^{+3} ions located in octahedral sites bonded to the carbons of CN groups, and also in complementary octahedral sites bonded to the nitrogen ends.[11] Raman and FTIR are less sensitive to Fe-O species and such groups may exist in the CCC, but cyano species other than H-bonded $Fe(CN)_6^{-3}$ and Berlin green are unlikely. If significant amounts of other cyano species are present, their C≡N stretching vibrations are not apparent in the IR or Raman spectra.

The reduction of Cr(VI) to Cr(III) by aluminum, whether direct or indirect, has long been accepted as a critical step in CCC formation. The role of ferricyanide in the process is less clear from the literature, although interference with Cr(VI) adsorption[5] and interactions with Cu containing intermetallics[6] have been proposed. The current results confirm that direct reduction of Cr(VI) in the absence of $Fe(CN)_6^{-3/-4}$ is quite slow, particularly for the AA 2024-T3 alloy. The results also establish that ferricyanide can act as a redox mediator by rapid reduction to ferrocyanide by the alloy, and rapid oxidation of ferrocyanide by Cr(VI), as depicted in Fig. 7. Ferricyanide has been used previously as a redox mediator for a variety of redox processes,[29,30] ranging from small molecules to redox enzymes. During CCC formation, several other redox systems can substitute for $Fe(CN)_6^{-3}$ as accelerators, although not as effectively. The rates of CCC film growth for the mediators tested followed the trend $Fe(CN)_6^{-3} > IrCl_6^{-2} > V^{+3} > Fe^{+3}$. However, this series does not correspond to the order of $E^{\circ\prime}$ values [$IrCl_6^{-3/-2} > Fe^{+3/+2} > Fe(CN)_6^{-3/-4} > V^{+3/+2}$]. This lack of correspondence implies that the kinetics of the redox cross reactions between Cr(VI), mediator and alloy have a larger effect on CCC growth rate than any tendency of the mediator to control the alloy potential at a value near the mediator's $E^{\circ\prime}$.

While the acceleration of CCC formation through redox mediation by $Fe(CN)_6^{-3/-4}$ is strongly supported by the current results, the possibility of other roles for $Fe(CN)_6^{-3/-4}$ in corrosion protection should be considered.[6] Given that the final film contains physisorbed $Fe(CN)_6^{-3}$ and Berlin green, are these components important to film behavior and corrosion protection? The chromate film formed with $IrCl_6^{-2}$ substituted for $Fe(CN)_6^{-3}$ is spectroscopically and visually very similar to a conventional CCC. It can release Cr(VI) into water, a process believed to be important to "self-healing" of the CCC.[23] The chromate film formed with $IrCl_6^{-2}$ also increases R_p and decreases the corrosion potential of AA 2024-T3, in much the same manner as a conventional CCC. Finally, the $IrCl_6$-formed film exhibits active protection by migration of released Cr(VI) to an initially untreated AA 2024 sample. At least by these tests, the chromate film formed in the absence of $Fe(CN)_6^{-3/-4}$ is visually, structurally, and functionally very similar to a conventional CCC. The current results do not rule out actions other than redox mediation by $Fe(CN)_6^{-3/-4}$, but they do establish that redox mediation accounts for the effect of $Fe(CN)_6^{-3}$ as an accelerator. Based on the tests used in the current work, $Fe(CN)_6^{-3}$ remaining in the CCC as Berlin green or physisorbed $Fe(CN)_6^{-3}$ is not necessary for higher polarization resistance, slower visual corrosion, or self-healing in the artificial scratch cell.

The behavior of intermetallic compounds (IMCs) is often invoked in explanations of corrosion mechanisms and protection by a CCC. For example, the formation of $Cu/Fe(CN)_6$ compounds at IMCs was proposed to decrease their reactivity and reduce corrosion.[6] The current spectroscopic observations were not resolved spatially, and hence the spectra represent spatial averages over 100-500 μm of a CCC or alloy surface. IMCs are present at levels of a few percent in particles smaller than this sampling area, so spectroscopic features resulting from IMC interactions with the CCC may contribute to the observed spectra in minor ways. It is possible that spectral features of the IMCs are lost in the relatively strong signal from the CCC itself. Both the IR and Raman spectra reflect major components of the CCC, and minor contributions may quite possibly be unobservable. The current results certainly do not rule out the possibility that effects related to IMCs, which represent a small fraction of the total IR or Raman spectra, may be important to corrosion protection by the CCC.

The existence of IMCs and other heterogeneities on the alloy surface raises a possibly important mechanistic role of ferricyanide. The variations in CCC thickness over intermetallic regions has been noted,[6] and it is possible that such variations degrade corrosion protection. With the $Fe(CN)_6^{-3}$ accelerator present, the reduction rate of Cr(VI) is greatly increased. More rapid generation of Cr(III) should result in more rapid formation of the hydrated chromium hydroxide film, and subsequent formation of a Cr(III)/Cr(VI) mixed oxide.[9] Rapid film formation may allow the CCC to grow over heterogeneities such as IMC's which normally resist CCC formation. The end result is a relatively homogeneous Cr(III)/Cr(VI) film covering an alloy surface which may itself be heterogeneous. The ability to form a uniform film by filling in surface heterogeneities through rapid Cr(III) generation may be a result of the accelerator which is quite important to ultimate corrosion protection.

Acknowledgments

This work was supported by the Air Force Office of Scientific Research, contract no. F49620-96-1-0479. The authors wish to thank Clive Clayton, Gerald Frankel, Gary Halada, and Martin Kendig for useful suggestions during the research.

The Ohio State University assisted in meeting the publication costs of this article.

References

1. F. W. Lytle, R. B. Greegor, G. L. Bibbins, K. Y. Blohowiak, R. E. Smith, and G. D. Tuss, *Corros. Sci.*, **37,** 349 (1995).
2. K. Asami, M. Oki, G. E. Thompson, G. C. Wood, and V. Ashworth, *Electrochim. Acta*, **32,** 337 (1987).
3. A. E. Hughes and R. J. Taylor, *Surf. Interface. Anal.*, **25,** 223 (1997).
4. J. A. Treverton and M. P. Amor, *Trans. Inst. Met. Finish.*, **60,** 92 (1982).
5. J. A. Treverton and N. C. Davies, *Surf. Interface Anal.*, **3,** 194 (1981).
6. P. L. Hagans, and C. M. Haas, *Surf. Interface Anal.*, **21,** 65 (1994).
7. M. W. Kendig, A. J. Davenport, and H. S. Isaacs, *Corros. Sci.*, **34,** 41 (1993).
8. J. K. Hawkins, H. S. Isaacs, S. M. Heald, J. Tanquada, G. E. Thompson, and G. C. Wood, *Corros. Sci.*, **27,** 391 (1987).
9. L. Xia and R. L. McCreery, *J. Electrochem. Soc.*, **145,** 3083 (1998).
10. A. M. Abern, P. R. Schwartz, and L. A. Schaffer, *Appl. Spectrosc.*, **46,** 1412 (1992).
11. D. B. Brown, D. F. Shriver, and L. H. Schwartz, *Inorg. Chem.*, **7,** 77 (1968).
12. K. Nakamoto, *Infrared and Raman Spectra of Inorganic and Coordination Compounds*, Part B, 5th ed., John Wiley & Sons, Inc., New York (1997).
13. M. W. Fuller, K-M F. Le Brocq, E. Leslie, and I. Wilson, *Aust. J. Chem.*, **39,** 1411 (1986).
14. G. Socrates, *Infrared Characteristic Group Frequencies*, John Wiley & Sons, New York (1994).
15. S. Hoste, L. Verdonck, and G. P. van der Kelen, *Bull. Soc. Chim. Belg.*, **7,** 91 (1982).
16. D. M. Drew, *Anal. Chem.*, **45,** 2423 (1973).
17. P. K. Dutta and M. Puri, *J. Phys. Chem.*, **93,** 376 (1989).
18. B. I. Swanson and J. J. Rafalko, *Inorg. Chem.*, **15,** 249 (1976).
19. N. R. de Tacconi, N. Myung, and K. Rajeshwar, *J. Phys. Chem.*, **99,** 6105 (1995).
20. K. Kunimatsu, *J. Electroanal. Chem.*, **262,** 195, (1989).
21. T. Ozeki and D. E. Irish, *J. Electroanal. Chem.*, **280,** 451 (1990).
22. Material Safety Data Sheet, Endura Manufacturing Co. Ltd. (1991).
23. J. Zhao, G. Frankel, and R. McCreery, *J. Electrochem. Soc.*, **145,** 2258 (1998).
24. M. A. Watzky, J. F. Endicott, X. Song, Y. Lei, and A. Macatangay, *Inorg. Chem.*, **35,** 3463 (1996).
25. A. Boffi and E. Chiancone, *Biochem.*, **36,** 4505 (1997).
26. G. Eaton, A. S. Dena-Nunez, and M. C. R. Symons, *J. Chem. Soc., Faraday Trans., 1*, **84,** 2181 (1988).
27. A. Simplerler and W. Mikenda, *Monatsh.Chem.*, **128,** 969 (1997).
28. P. S. Braterman, C. Tan, and J. Zhao, *Mater. Res. Bull.*, **29,** 1217 (1994).
29. P. Jeroschewski, K. Haase, A. Trommer, and P. Grundler, *Electroanalysis*, **6,** 769 (1994).
30. S. Uchiyama, Y. Kurokawa, Y. Hasebe, and S. S. Suzuki, *Electroanalysis*, **6,** 63 (1994).